Unification of the low-energy excitation peaks in the heat capacity that appears in clathrates

Jiazhen Wu,[1] Kazuto Akagi,[2] Jingtao Xu,[3] Hidekazu Shimotani,[1] Khuong K. Huynh,[2] and Katsumi Tanigaki[2,1,*]

[1]*Graduate School of Science, Tohoku University, Sendai 980-8578, Japan*

[2]*WPI-AIMR, Tohoku University, Sendai 980-8577, Japan*

[3]*Ningbo Institute of Materials Technology & Engineering, Chinese Academy of Sciences, Ningbo 315201, China*

(Received 16 October 2015; revised manuscript received 18 February 2016; published 9 March 2016)

We report that anomalous low-energy excitation (ALE) peaks in the heat capacity emerging from single-crystal cage materials can be successfully rationalized in terms of a single unified exponential line for a variety of type-I clathrates by employing a parameter associated with the freedom of space and the modified radii of guest atoms estimated by band calculations. The origin of these low-energy excitations is interpreted in the framework of quasiharmonic van der Waals type guest-host interactions based on a unified picture with the help of first-principles calculations. It is shown that the influence of guest-host ionic and covalent bonding interactions on the phonon anharmonicity, which have so far been considered to play an important role, are not significant as long as high symmetry of the cage structure is preserved. The dominant van der Waals interactions explain the soft vibrational modes of the rattling, which suppress phonon transport and lead to the concept of "phonon-glass electron-crystal" (PGEC) for thermoelectric applications. A few exceptions existing in type-I clathrates, as indicated by deviations from the unified line, suggest that a quasiharmonic potential can become more asymmetric via lower symmetry of the cage structure, towards glasslike disordered states at even lower temperatures. Although the origin of the boson peaks appearing in disordered materials is still under debate due to incomplete information on the real structure, the understanding provided by the present paper for crystalline cage materials may provide information partly applicable to other disordered systems.

DOI: 10.1103/PhysRevB.93.094303

I. INTRODUCTION

Anomalous low-energy excitation (ALE) peaks have frequently been observed in glasslike materials such as amorphous silica at terahertz (THz) frequencies (at an energy level of around 50 K) by various experimental methods [1–4]. These peaks, associated with strong phonon anharmonicity, are generally referred to as boson peaks in the case of a disordered glass system [1–5]. Another recent front-line research finding is that similar ALE peaks can also be observed even in single crystal materials having cage structures containing guest atoms, such as clathrates, pyrochlores, skutterudites, brownmillerites, and $Al_{10}V$ type intermetallides [6–11]. In contrast to the situation of glasses, these cage-structured materials can be categorized as single crystals with higher symmetry, and the ALE peaks can be described by an additional quasiharmonic (QH) oscillation mode associated with on-centered guest-atoms inside of a cage, except for a few type-I clathrates showing larger anharmonicity with off-centered guest atoms, such as $Sr_8Ga_{16}Ge_{30}$ (SGG), $Eu_8Ga_{16}Ge_{30}$ (EGG), and $Ba_8Ga_{16}Sn_{30}$ (BGSn) [12,13] as well as type-III $Ba_{24}Ge_{100}$ [14]. Over the last two decades, these ALE (QH and AH) peaks in clathrates have been shown to be important in phonon transport for providing low thermal conductivity while keeping relatively high electrical conductivity [6,15–17], the phenomenon is known as the concept of "phonon-glass electron-crystal" (PGEC) [18]. Similar cage compounds, such as skutterudites and pyrochlores, can also be classified as the conceptual materials for PGEC because of their ALE phonon modes (called rattling phonon modes), and have also been studied from the viewpoint of applications in thermoelectrics, in addition to having other intriguing physical properties such as superconductivity [14,19].

Although QH and AH phonons characterized by ALE peaks clearly play a significant role in the PGEC concept in cage materials, a complete understanding is still under debate, and a systematic study of a variety of cage materials has not been fully attempted. Among the many candidates of single-crystal cage compounds, type-I clathrates are considered to be most suitable, since a variety of cage structures as well as many kinds of guest atoms accommodated in the cage from the periodic table—starting from alkali metals (A), alkaline earth metals (E), and some rare-earth metals (R)—can be synthesized, allowing for a wide range of free accommodation space inside the cage as shown in Fig. 1. Importantly, in type-I clathrates, which are different from many other cage compounds, the phonon modes vary from harmonic (H) to QH and to anharmonic (AH) when approaching a strong disordered mode, and therefore a systematic study may provide useful information for understanding the boson peaks observed in a disordered system.

In the present paper, we show that many scattered experimental data concerning ALE peaks in type-I clathrates can be successfully unified in terms of a well-correlated single universal line with an exponential function, by plotting their force constants as a function of a free space parameter introduced for the atoms accommodated inside the cage (R_{free}) and the van der Waals radii evaluated by first-principles band calculations. The influence of ionic Coulombic and covalent bonding interactions between the elements constituting a cage and the guest atoms inside the cage on the ALE peaks are discussed on the basis of a unified relationship, with the help of a van der Waals potential model using a Morse type potential and first-principles calculations.

*Corresponding author: tanikagi@sspns.phys.tohoku.ac.jp

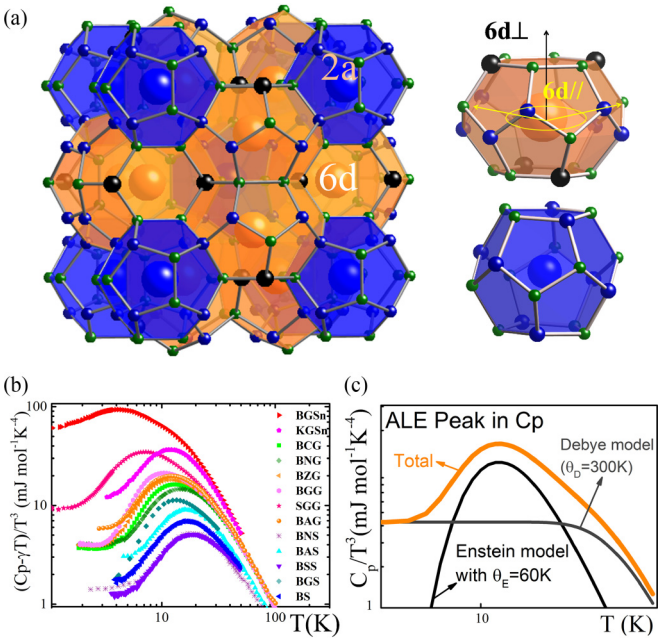

FIG. 1. (a) The crystal structure of type-I clathrates, which contains two kinds of cages: two dodecahedral (blue) and six tetrakaidecahedral (orange) cages in a unit cell. The vibration modes of guest atoms inside the larger tetrakaidecahedral cages are schematically shown by arrows with different colors: black arrow: perpendicular modes to a six-membered ring plane; yellow arrows: parallel modes to a six-membered ring plane. (b) Experimental data of ALE peaks in C_p appearing at around 10 K in type-I clathrates (see the experimental method for a description of the compounds). (c) Evolution of ALE peaks deconvoluted by using harmonic (H) Debye and Einstein models.

II. EXPERIMENT AND CALCULATION METHODS

Single crystals of type-I clathrates, SGG, $Ba_8Ga_{16}Ge_{30}$ (BGG), $Ba_8Zn_8Ge_{38}$ (BZG), $K_8Ga_8Sn_{38}$ (KGSn), and BGSn, were synthesized by a Ga, Sn, or Zn flux method as reported previously [20,21]. The quality of single crystals was confirmed by single crystal x-ray diffraction and electron probe microanalysis. Polycrystal compounds including $Ba_8Cu_{5.3}Ge_{40.7}$ (BCG), $Ba_8Ag_{5.3}Ge_{40.7}$ (BAG), and $Ba_8Ni_4Ge_{42}$ (BNG) were prepared by using a radio frequency (RF) induction furnace. These compounds were confirmed by x-ray powder diffraction as previously described [22]. Heat capacity measurements were carried out by using a Quantum Design physical property measurement system (PPMS) for the selected compounds described above. The C_p data of $Ba_8Au_{6.1}Si_{39.9}$ (BAS), $Ba_8Ni_{3.8}Si_{42.2}$ (BNS), Ba_8Si_{46} (BS), $Ba_2Sr_6Si_{46}$ (BSS), $Ba_8Ga_{16}Si_{30}$ (BGS), Na_8Si_{46} (NS), and $Sr_8Ga_{16}Si_xGe_{30-x}$ (SGSG) are taken from Refs. [23–28].

The GAUSSIAN 09 program [29] was used to calculate the vibrational frequencies of the guest atoms inside the 24-cages of ASi_{24}, where A is Sr, Ba, Na, K, Rb, or Cs, as well as inner gas elements He, Ne, Ar, Kr, or Xe. The structures were optimized using density functional theory with the Becke's three-parameter hybrid functionals [30] with the Lee-Yang-Parr correlation functional [31] (B3LYP). The 6-31G* basis set was used [32] for atomic numbers not larger than 36 (Kr), while for heavier elements the LANL2DZ basis set [33] with pseudopotential was used.

First-principles calculations were made using the Vienna Ab-initio Simulation Package (VASP) program [34]. Projector augmented wave (PAW) type pseudopotentials [35,36] and the density functional GGA-PBE (Perdew-Burke-Ernzerhof parametrization of the generalized gradient approximation) [37] were used for description of the electronic state. The planewave basis set with cutoff energy of 700 eV and $4 \times 4 \times 4$ Monkhorst-Pack k-point meshes were applied to the $1 \times 1 \times 1$ unit cell (X_8Si_{46}). The lattice constant was set to 1.041 nm, which shows the minimum total energy for the Ba_8Si_{46} system within the above calculation condition. Structure optimization was done under BCC symmetry with the convergence criterion of $\Delta E = 1.0$ meV.

III. RESULTS AND DISCUSSION

A. Analyses on the anomalous low-energy excitation (ALE) peaks in C_p data

Normally, the heat capacity C_p in solids can be described as a function of temperature (T) in the framework of harmonic approximation as $C_p = C_{ph} + \gamma T = C_D + C_E + \gamma T$, where C_D and C_E are the lattice heat capacities (C_{ph}) contributed to by the Debye and the Einstein modes, respectively, and γT results from the contribution of the itinerant conduction carriers of the electrons and holes as well as tunneling states of the AH phonons, as discussed elsewhere [20,21]. Each term can be given as

$$C_D = 9N_D k_B \left(\frac{T}{\theta_D}\right)^3 \int_0^{x_D} dx \frac{x^4 e^x}{(e^x - 1)^2}, \quad (1)$$

$$C_E = 3N_E k_B \frac{x_E^2 e^{x_E}}{(e^{x_E} - 1)^2}, \quad (2)$$

where N_D and N_E are the number of vibration modes for the Debye and the Einstein terms, respectively, k_B is the Boltzmann constant, and θ_D is the Debye temperature. The value of x can be defined as $x \equiv \hbar\omega/k_BT$, with the following notation: $\hbar$ the reduced Plank constant, ω the oscillator frequency, $x_D = \hbar\omega_D/k_BT$ at the Debye cutoff frequency ω_D, and $x_E = \hbar\omega_E/k_BT$ at the Einstein oscillator frequency ω_E. In a common crystalline material, C_{ph} can be described by the Debye T^3 law at low T, as C_E is negligibly small in the low-T limit. However, an excess amount of additional C_E is observed as ALEs in clathrates, which violates the T^3 law and creates ALE peaks at around 10–20 K, as can be seen clearly in the plot of C_p/T^3 as a function of T (Fig. 1).

Reasonably good fitting can be achieved for the experimental C_{ph} data by applying the model described earlier as shown in Fig. 2(a). Here, the 6d parallel modes with the lower excitation energy ω_{E1} and the 6d vertical modes with the higher energy ω_{E2} were considered for the Einstein modes for analyses, while the 2a modes were treated in the conventional manner [see Fig. 1(a)]. According to the cage structure, there are in principle twelve modes in the 6d parallel directions and six modes in the 6d vertical directions of a unit cell. Generally, the 6d parallel modes dominate the peaks, while the 6d vertical modes contribute less than 10%, as can be seen in Fig. 2(a). In the actual fitting, we set $N_{E2} = 6$ and left N_{E1}

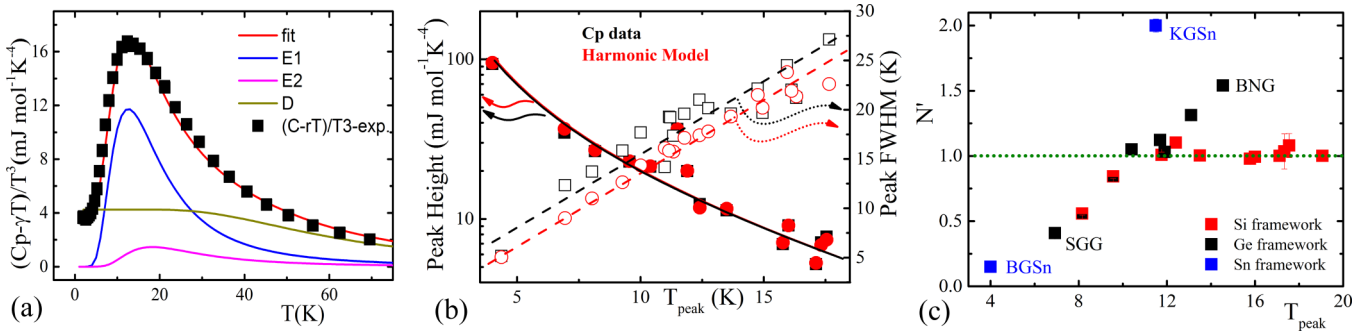

FIG. 2. (a) C_p of a typical type-I clathrate of BCG and its deconvoluted components as described in the text. D represents the Debye model and E1 and E2 represent the Einstein model with two different frequencies ω_{E1} and ω_{E2}, respectively. (b) Peak height and full width at half maximum (FWHM), obtained from analysis of the experimental data. The solid curves and the dashed lines (red and black in color) serve as guides for the eyes. (c) Relationship between the normalized number of 6d parallel modes N' and the peak temperatures T_{peak}.

as a free variable. The fitting results are given in Figs. 2(b) and 2(c), and the fitting parameters are summarized in Table I. For most of the compounds, the present models show consistent peak heights, full widths at half maximum (FWHM), and T_{peak} with the experimental data, as shown in Fig. 2(b). The model employed here describes well the C_p of these materials as a QH system. It should be noted that the peaks of the experiment data were slightly wider than those calculated from the model, and the differences are considered to be due to the more complex situation in the real materials compared to what is described by the present model.

TABLE I. The parameters used in fitting, θ_{E1}, θ_{E2}, θ_D and N', for the C_p data shown in Fig. 1(b). Abbreviations of clathrates are BS: Ba_8Si_{46}; BGS: $Ba_8Ga_{16}Si_{30}$; BAS: $Ba_8Au_xSi_{46-x}$; BNS: $Ba_8Ni_{3.8}Si_{42.2}$; BAG: $Ba_8Ag_{5.3}Ge_{40.7}$; SGG: $Sr_8Ga_{16}Ge_{30}$; BGG: $Ba_8Ga_{16}Ge_{30}$; BZG: $Ba_8Zn_8Ge_{38}$; BNG: $Ba_8Ni_4Ge_{42}$; BCG: $Ba_8Cu_{5.3}Ge_{40.7}$; SGSG: $Sr_8Ga_{16}Si_xGe_{30-x}$; KGSn: $K_8Ga_8Sn_{38}$; BGSn:$Ba_8Ga_{16}Sn_{30}$; NS: Na_8Si_{46}; and KS: K_8Si_{46}. The numbers in parentheses are the x values corresponding to $Ba_8Au_xSi_{46-x}$ and $Sr_8Ga_{16}Si_xGe_{30-x}$, respectively. A: ADP; R: Raman; I: INS.

Compound	θ_{E1} (K)	θ_{E2} (K)	θ_D (K)	N'	Ref. θ_{E1} (K)
BS	76	110	372	1.0	71 (R) [40]
BGS	63	107	330	1.1	63 (R) [41]
BAS(6.1)	74	95	326	1.0	73 (C_p) [23]
BAS(5.6)	78	84	343	1.0	76 (C_p) [23]
BAS(4.9)	79	94	353	1.1	78 (C_p) [23]
BAS(4.1)	80	101	358	1.0	79 (C_p) [23]
BNS	87	109	399	1.0	91 (A) [24]
BAG	56	83	250	1.1	54 (I) [42]
SGG	33	80	196	0.4	35 (C_p) [27]
BGG	50	80	278	1.0	50 (R) [43]
BZG	56	84	280	1.2	56 (I) [44]
BNG	70	85	282	1.5	63 (I) [44]
BCG	62	82	281	1.2	57 (I) [44]
SGSG(30)	60	110	370	1.1	59 (C_p) [27]
SGSG(25)	58	112	317	1.0	56 (C_p) [27]
SGSG(10)	47	106	241	0.8	46 (C_p) [27]
SGSG(5)	40	82	220	0.6	41 (C_p) [27]
KGSn	57	90	191	2.0	65 (A) [45]
BGSn	20	75	118	0.2	20 (C_p) [13]
NS	106	147	560	1.0	94 (C_p) [28]
KS					120 (R) [46]
Rb_8Sn_{44}					49 (R) [47]
Cs_8Sn_{44}					36 (R) [47]
$Rb_8Hg_4Sn_{42}$					43 (R) [47]

The number of the normalized *6d* parallel modes $N' = N_{E1}/12$ is plotted as a function of T_{peak} in Fig. 2(c). The values of N' are around 1 for almost all compounds with on-centered guest atoms, except for a few compounds of KGSn and BNG showing values of 2 and 1.5, respectively. N' values higher than 1 indicate that the *6d* parallel modes are mixed with other modes due to their similar energies, and the additional modes result from the acoustic branches near the Brillouin zone boundaries as the acoustic dispersion curve is strongly flattened around these areas. On the other hand, N' much smaller than 1 was obtained for the compounds showing off-centered guest atoms as well as glasslike properties [12,38], as in the case of BGSn with $N' = 0.2$ and SGG with $N' = 0.4$. The reduction in the number of modes frequently happens when the Einstein mode energies are suppressed to very low values (indicated by T_{peak}) and the phonons become more anharmonic. Although the understanding of the physical origins of the ALE peaks is not satisfactory, the newly defined parameter N' seems to represent the strength of phonon anharmonicity in type-I clathrates, and it could also indicate an evolution from H to QH and to AH, i.e., a tendency towards a disordered system. It should be noted, however, that the present model cannot be sufficient for yielding a detailed understanding of BGSn and SGG with off-centered atoms in the cage [38]. Generally, more complex models such as the soft potential model and the modified analyses based on the Debye-Einstein harmonic model including Anderson's two level tunneling or Nakayama's dipole-dipole interaction are frequently applied [4,20,21,38,39]. However, as far as the present discussion is concerned, the present analytical fitting is sufficient. It should be noted that, although there might be some errors in the present analyses on C_p, the fitting results are reliable as they are also consistent with the experimental data obtained from inelastic neutron scattering (INS), Raman scattering, and the Debye-Waller thermal factors obtained from x-ray–neutron diffraction. Our studies mainly focus on θ_{E1}, and the θ_{E1} obtained from other studies are also listed in Table I for comparison.

It will be discussed later that the guest-host interactions are mainly limited inside the cage and the low-energy excitation

TABLE II. Theoretical calculations of vibration frequencies and corresponding F_c's. The cages from $SrSi_{24}$ to $XeSi_{24}$ are calculated by the GAUSSIAN 09 code, while compounds BS(x) as a function of contraction of cell parameter are calculated by the vasp program.

Name	ω (cm^{-1})	F_c (mdyn/Å)
$SrSi_{24}$	62.7	0.200
$BaSi_{24}$	52.8	0.228
$NaSi_{24}$	81.1	0.088
KSi_{24}	92.5	0.197
$RbSi_{24}$	68.2	0.234
$CsSi_{24}$	60.8	0.258
$HeSi_{24}$[a]	99.1	0.023
$NeSi_{24}$	64.4	0.050
$ArSi_{24}$	82.0	0.158
$KrSi_{24}$	57.3	0.162
$XeSi_{24}$	51.5	0.205
BS(100)[b]	57.3	0.266
BS(99)	61.4	0.306
BS(98)	65.3	0.346
BS(97)	69.2	0.389
BS(96)	72.9	0.431
BS(95)	76.6	0.476
BS(94)	79.4	0.512

[a]Clathrates containing inert gas elements He, Ne, Ar, Kr, and Xe have not yet been successfully synthesized. However, in the present work, for our extended discussion we calculated the low-energy oscillation frequencies for the cluster models of the larger 24-cages containing these elements as guest atoms using the GAUSSIAN 09 code.

[b]For further clarification of the importance of the space, the lattice of Ba_8Si_{46} (BS) was hypothetically contracted from 100% to 94% and the low-excitation vibrational frequencies were calculated

peaks mainly arise from oscillations of the atoms accommodated in the larger 24-cages in the parallel direction. The influence from the other atoms outside of the cage becomes negligibly small because such additional forces can cancel each other due to the high symmetry of the crystal. It is also important that other interactions that can be given to create potentials inside of a cage, such as ionic, Coulombic, and covalent interactions, can cancel each other as long as the high symmetry of a host cage structure is preserved, as will be discussed later. For an extended discussion including a variety of elements accommodated in a cage structure, we calculated the oscillation frequencies of the guest atoms based on a cluster model by employing the GAUSSIAN 09 code. The results are summarized in Table II

B. Unified picture of the low excitation energy peaks

The ALE peaks originating from the oscillations of guest atoms in a cage compound are supposed to depend on the space for freedom and the mass of the encapsulated atom. In order to clarify their features, we tentatively plotted the specific energies of the peaks (θ_E, which only focuses on the 6d parallel modes), in units of temperature (K), as a function of either cage radius (R) in Fig. 3(a) or mass (m) of an atom accommodated inside a cage in Fig. 3(b). Here, the cage radius R is defined as the distance between the center of the cage and the nearest atom residing on the larger host 24-cages [see Fig. 1(a)]. As can clearly be seen in Fig. 3(a), the peak energies are strongly reduced as the R parameter increases. It is also apparent that, at the same time, the energies depend on the mass of guest atoms, as shown in Fig. 3(b). Intriguingly, the kind of atoms constituting the host cage structure seems to have nearly no influence on the peak energies. The experimental fact, deduced from these two fundamental parameters, suggests that the origin of the low-excitation energies in clathrates may be less complex than we had originally considered.

In order to observe clear correlations between the low-energy peaks and the free space inside of a cage, a parameter associated with the free space (R_{free}) was introduced in place of R. We defined the free space as $R_{\text{free}} = R - R_{\text{g}} - R_{\text{h}}$, where g and h stand for an accommodated guest and host-cage atoms, respectively [13,20] [see Fig. 3(f). Other definitions can express the freedom of the space inside the cage; one can see that the definition made here is very convenient for association with the potential model described later. The mass m of an atom accommodated in a cage can be used in place of the reduced mass [$\mu = Mm/(M+m)$], because the cage framework mass (M, as the sum of a number of atoms residing on a cage) is much larger than m ($M \gg m$). To describe the ALE peak energies, we used the force constant F_c, where the mass [$F_c = (\theta_E)^2 m$] can be renormalized under a two-body harmonic oscillator model. Since the space inside the 24-cage, as estimated previously [20], is indeed large, van der Waals type interactions appear to be dominant between the guest atoms and the cages. Actually, the evaluated F_c's are comparable to those of the conventional van der Waals interactions. For instance, the F_c is known to be about 0.03 mdyn/Å for Ar-HF in a pure van der Waals crystal [48]. These values can be compared to those of the strong covalent interactions, where the F_c's are generally of the order of 10 mdyn/Å [49]. Therefore, to interpret the data, we tentatively employed van der Waals radii (R_{vdW}) given in the literature [50–52] for both R_{g} and R_{h}. The values used values are 1.625 Å (Sr^{2+}), 1.802 Å (Ba^{2+}), 1.352 Å (Na^{+}), 1.671 Å (K^{+}), 1.801 Å (Rb^{+}), and 1.997 Å (Cs^{+}) for ions; and 1.40 Å (He), 1.54 Å (Ne), 1.88 Å (Ar), 2.02 Å (Kr), 2.16 Å (Xe), 2.10 Å (Si), 2.11 Å (Ge), 2.17 Å (Sn), 1.87 Å (Ga), 1.39 Å (Zn), 1.4 Å (Cu), 1.63 Å (Ni), 1.72 Å (Ag), 1.66 Å (Au), and 1.55 Å (Hg). We note that the R_{vdW} values listed in the table were the ones optimized suitably for a general system, and the actual R_{vdW} values for clathrates are possibly different.

The relationship between F_c and the parameter R_{free} is shown in Fig. 3(d). Interestingly, the experimental data fall into three groups: inert gas (G), alkali metal (A), and alkaline earth metal (E), respectively. The three data sets are fitted well by exponential functions $F_c = C\exp(-3.0R_{\text{free}})$, with C equal to $(7.53 \pm 0.15) \times 10^{-2}$ mdyn/Å for E elements, $(4.97 \pm 0.43) \times 10^{-2}$ mdyn/Å for A elements, and $(1.98 \pm 0.19) \times 10^{-2}$ mdyn/Å for G elements.

A great surprise at this stage is that all three groups were approximately described by the same exponential function of $\exp(-3.0R_{\text{free}})$ with only small differences in the prefactors of C. This is not coincidental and strongly suggests that the three curves might be unified as a single-curve relationship. In order to search for such unification of these three lines (for E, A, and G elements), one could take two different positions.

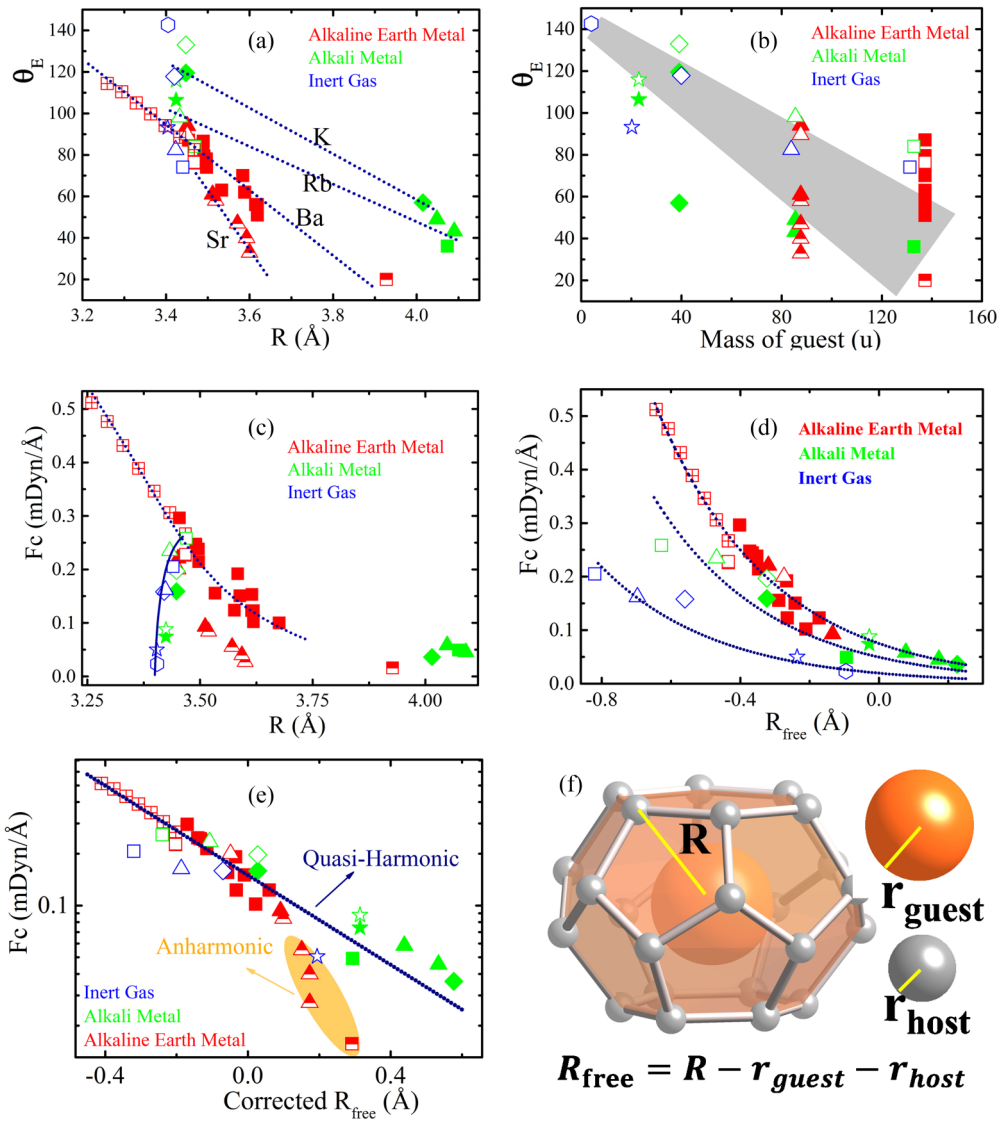

FIG. 3. Excitation energies of guest atoms in type-I clathrates as a function of space parameters. (a) The relationship between θ_E (the lowest specific temperature of θ_{E1}, used in the whole article) and R. The dotted lines are guides for the eyes. (b) The relationship between θ_E and the mass of the guest elements (m). The grey shadow is a guide for the eyes. (c) The relationship between F_c and R. The dotted line and the solid line serve as guides for the eyes. (d) The relationship between F_c and R_{free}, as defined in the text. The lines are fitting results by employing exponential functions. (e) The relationship between F_c and the corrected R_{free}, with a logarithmic scale of the ordinate, by applying the radii of the guest atoms evaluated from first-principles calculations. (f) The definition of R_{free}. Legends: hexagon: He; star: Ne and Na; diamond: Ar and K; up triangle: Kr, Rb, and Sr; square: Xe, Cs, and Ba. The empty symbols and the ones with a cross inside are theoretical calculations evaluated by GAUSSIAN 09 [29] and VASP [34], respectively. The half-filled symbols are compounds showing guest-atom off-centered behavior. All data sets are given in the tables.

The first one is that the different prefactors have a physical meaning, and they may originate from additional interactions, such as ionic interactions, covalent interactions, and other special interactions associated with confinement, which are not taken into account in the present discussion. The second is that the van der Waals radii employed in literature to evaluate R_{free} are not sufficiently suitable parameters for describing the clathrate systems that contain cage structures. We show in the following paragraph by employing first-principle calculations that the second interpretation is correct and that the ionic interactions, generally considered to be important, exert little influence.

It is important to know that van der Waals interactions should seriously be taken into consideration even in ionic species, as described in many reports and discussions [52]. In the present paper, the guest atom radii (R_g) applicable to clathrates were theoretically reevaluated by applying first-principles calculations. We calculated electron density contour maps for various clathrates, as shown in Fig. 4. One can see that the radii can be evaluated by the boundary where the wave function shows a sharp change in the electron density map. The guest radii were carefully determined by the red contour zone of the electron density map appearing when the cutoff level for viewing the density map is changed. The values were

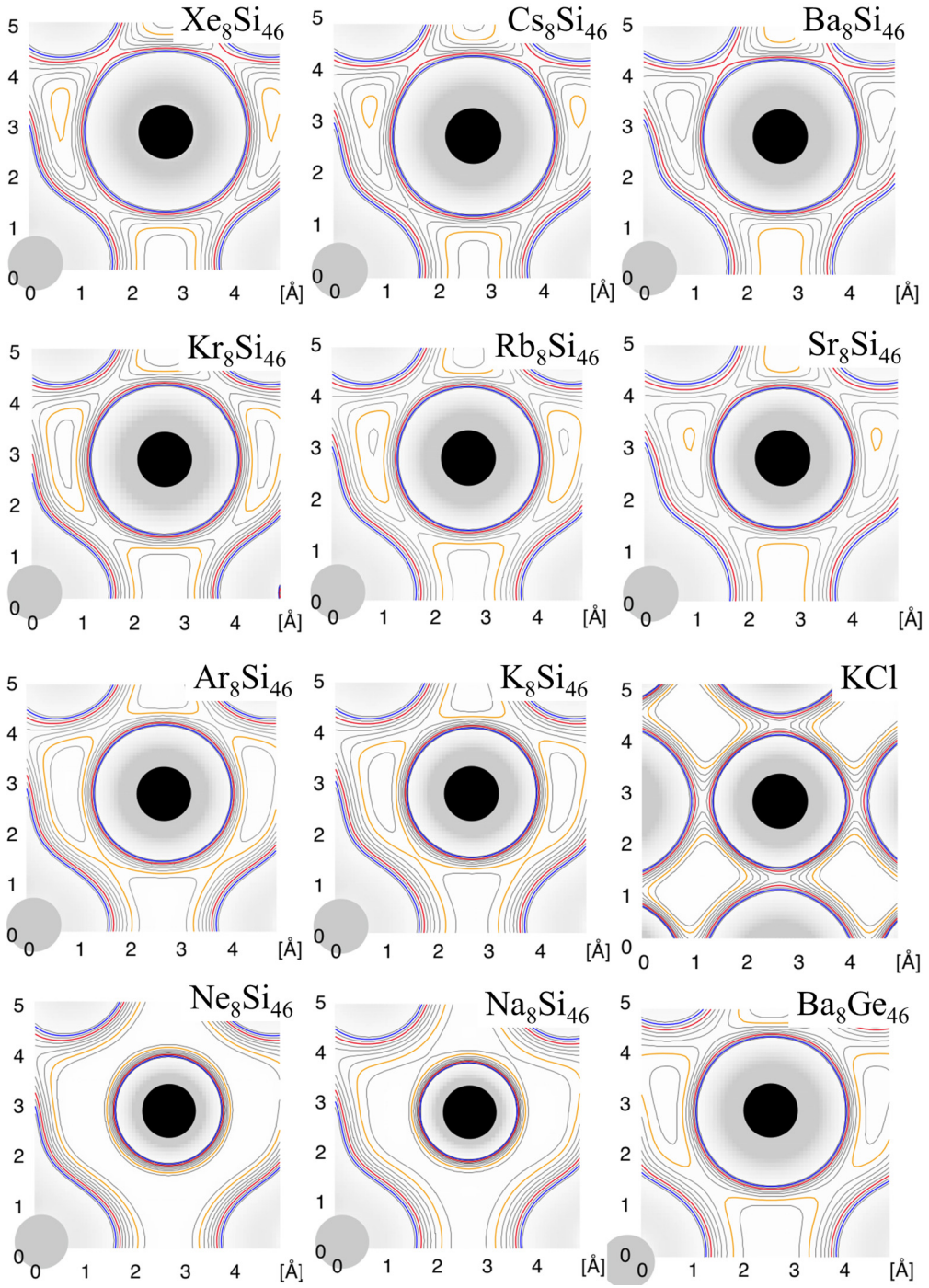

FIG. 4. The electron density counter maps for various clathrates, A_8Si_{46} (A = Ba, Sr; Cs, Rb, K, Na; Xe, Kr, Ar, Ne) and Ba_8Ge_{46}, in addition to KCl for comparison.

deduced to be 1.57 Å (Ba in Ba_8Si_{46}), 1.54 Å (Ba in Ba_8Ge_{46}), 1.40 Å (Sr), 1.61 Å (Cs), 1.44 Å (Rb), 1.32 Å (K in K_8Si_{46}), 1.01 Å (Na), 1.66 Å (Xe), 1.51 Å (Kr), 1.39 Å (Ar), 1.11 Å (Ne), and 1.36 Å (K in KCl).

It should be noted that the evaluation method of the radii using the equivalent electron density contour map can also provide a good conceptual image of the free space inside a cage. To our surprise, it was found that three exponential lines can be successfully unified as a single universal line, when R_{free} is reevaluated using the new values of R_g as shown in Fig. 3(e). Note that the relationship is expressed on a logarithmic scale so that correlations can clearly be seen. The unified exponential curve, $F_c = 0.15\exp(-3.0R_{\text{free}})$ was successfully deduced from the data, except for only a few compounds such as BGSn, SGG, and SGSG [27], with small but obvious deviations, showing extremely strong anharmonicity of guest vibrations, as shown by the half filled symbols in Fig. 3(e). Similar to N' described earlier, the unified picture can be another indicator

of the anharmonicity in phonons as well as the transition from a crystalline system to a glasslike disordered system.

This unified exponential relationship gives the following important conclusions on ALE peaks in clathrates. (1) The most important interaction contributing to ALE peaks in clathrates is the weak repulsive van der Waals interaction. It is shown later that the anharmonic terms resulting from the potential are considerably smaller than the harmonic terms, and the system can be classified as a quasiharmonic system. The van der Waals interactions are the origin of the soft modes of guest atoms in clathrates with guest on-centered elements inside a cage, which show anharmonicity categorized in the QH mode described earlier. (2) Neither Coulombic nor covalent bonding interactions have a large influence on ALE peaks. This is slightly contradictory to previous reports [53], but can be justified by first-principles band calculations (shown later). (3) Beyond the QH nature of the guest anomalous vibrations in clathrates, the existence of guest off-centered behavior associated with stronger anharmonic guest-atom oscillations observed in a few clathrate compounds (such as SGG and BGSn) is strongly indicative of the fact that, in addition to the dominant van der Waals interactions, weak guest-host ionic [13,45] or covalent [54,55] interactions may exert influences and lead to a lower or broken symmetry and yield larger anharmonicity of phonons. As long as the high symmetry of a cage is preserved, Coulombic and covalent interactions between guest atoms and the constituent elements of a cage will cancel out and the their influences will be negligibly small, as can be seen in the first-principle calculations later. Such lower symmetry as well as disorder can be created by the rearrangement of the elements residing on the host cage in the case of clathrates, as suggested earlier for BGG and SGG based on high-energy photoelectron spectroscopy [56] and extended x-ray absorption fine structure (EXAFS) [57] studies, and therefore some ternary-component clathrates shown by the half-filled symbols in Fig. 3(e) display a tendency, approaching stronger anharmonic vibrations, of showing much lower F_c, even though the R_{free} is not the largest among the clathrates studied here. Given lower symmetry as well as sufficient free space of the guest atoms, hidden ionic and/or covalent attractive interactions eventually emerge and the guest atoms are off-centered at the same time [13,45,54,55]. Under these circumstances, ALE peaks categorized in the AH mode emerge at extremely low temperatures of generally less than 1 K, one order lower than that in the QH mode, in the case of clathrates. The lowering of symmetry in structures with large free space is essentially important for strong anharmonicity in ALE peaks [38,56,58,59] and this is also the case for glasslike disordered materials.

C. Interpretations by theoretical calculations

It has been described so far that the ALE peaks, arising from the atomic vibrations with large freedom inside the cage, can be interpreted as a consequence of weak van der Waals repulsive interactions between the guest atoms and the host cage atoms. Now we provide an important justification by first-principles calculations and a potential model based on van der Waals interactions.

In order to judge how we should consider ionic interactions, we performed calculations using the VASP program [34]. First, we calculated the electron density distribution and the guest vibration frequencies for Ne_8Si_{46}, K_8Si_{46}, and Ba_8Si_{46}. The electron density difference maps in one unit cell are shown in

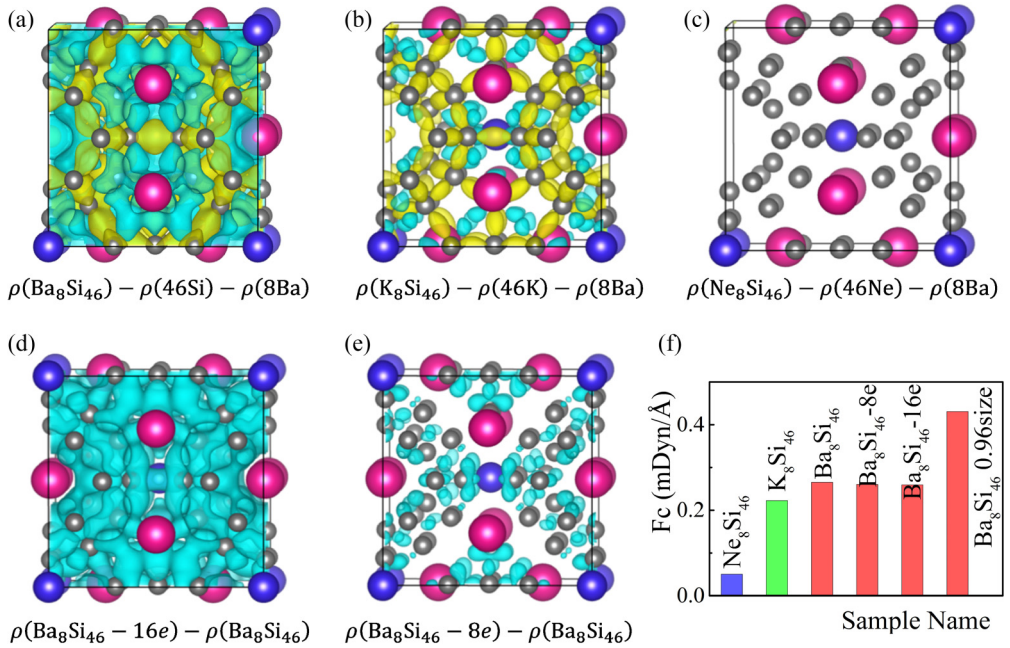

FIG. 5. Electron density difference maps and the corresponding F_c, calculated using the VASP code. Red and blue spheres represent the guest atoms at nonequivalent sites. Gray spheres represent Si atoms. (a)–(c) Charge redistribution with the introduction of guest atoms in Ba_8Si_{46}, K_8Si_{46} and Ne_8Si_{46}, where the blue region is electron decreased and the yellow region is electron increased. (d),(e) Difference in spatial charge density (electron-decreased region) between positively charged (+8 and +16) and neutral systems. (f) A comparison with the calculated F_c.

Figs. 5(a)–5(c), and the F_c estimated for the 6d parallel modes are shown in Fig. 5(f). These calculations provide important information regarding how the ionic states of divalent (Ba^{2+}), monovalent (K^+), and zero-valent (Ne^0) guest atoms affect the interaction strength. At first glance, an electron is transferred from the guest atoms to the host cage frameworks as can be visualized in Figs. 5(a)–5(c) by blue (electron-decreased) and yellow (electron-increased) regions. For instance, one electron or two electrons are transferred from K or Ba to the Si_{46} cage network in the case of Ba_8Si_{46} and K_8Si_{46}, respectively, while negligible electron transfer was detected for Ne_8Si_{46}. Meanwhile, the calculated F_c's, which are quantitatively in good agreement with the values used in Fig. 3, become smaller from Ba to K and to Ne, as can be seen in Fig. 5(f). One may imagine that the guest valences may have some influence on the guest-host interactions; however, this conclusion is not correct as we shall see in the following paragraph.

We performed additional calculations supposing a different situation in order to clarify the charge influence. Eight or sixteen electrons were hypothetically removed from the Si_{46} cage network in Ba_8Si_{46} in the first step. Structure optimization with constraints on the same lattice parameter shows no significant displacement of atoms in both systems. The electron density difference and the corresponding F_c were calculated for Ba_8Si_{46} ($-16e$) and Ba_8Si_{46} ($-8e$), respectively, as shown in Figs. 5(d), 5(e), and 5(f). Almost the same maps were obtained with $\sum|\psi_{\mathrm{LUMO}+i}(r)|^2$ ($i = 0$ to 3 for $-8e$ and $i = 0$ to 7 for $-16e$; $\Psi(r)$ is a kohn-Sham orbital; LUMO denotes lowest unoccupied molecular orbital) of the neutral Ba_8Si_{46}. Strikingly, the frequencies of the guest vibrations have a negligible dependence on these hypothetical charge variations, as shown in Fig. 5(f). These calculations clearly demonstrate that the Coulombic ionic interactions do not make a significant contribution to the excitation peaks. Therefore the different F_c's shown in Fig. 5(f) should be ascribed to the free space of the guest atoms associated with van der Waals radii rather than their charge valences.

For further understanding, we calculated the F_c when the lattice of Ba_8Si_{46} is hypothetically contracted up to 0.94a, where a is the cell parameter. Importantly, the F_c evaluated by first-principles band calculations under a hypothetical high pressure fall on the unified line fairly well, as shown in Fig. 3(e). This fact also supports our interpretation that the potential inside a cage can predominantly be controlled by the repulsive van der Waals interactions between a guest atom and the cage framework.

D. A potential model

The energy potential in a system consisting of two atoms, which interact with each other via van der Waals interactions, can be described by using a modified Morse potential [60] given by $V(r) = ae^{-nb(r-r_e)} - ane^{-b(r-r_e)}$, where r is the distance of the two atoms and r_e is their equilibrium distance; n, a, and b are free parameters with $n \gg 1$ to create a stable potential. The first and the second terms correspond to repulsive and attractive interactions, respectively. Given a situation in which two identical atoms located in a host cage framework separated by a distance of 2R (the radius of a cage is R) and a guest atom located on the line connecting these

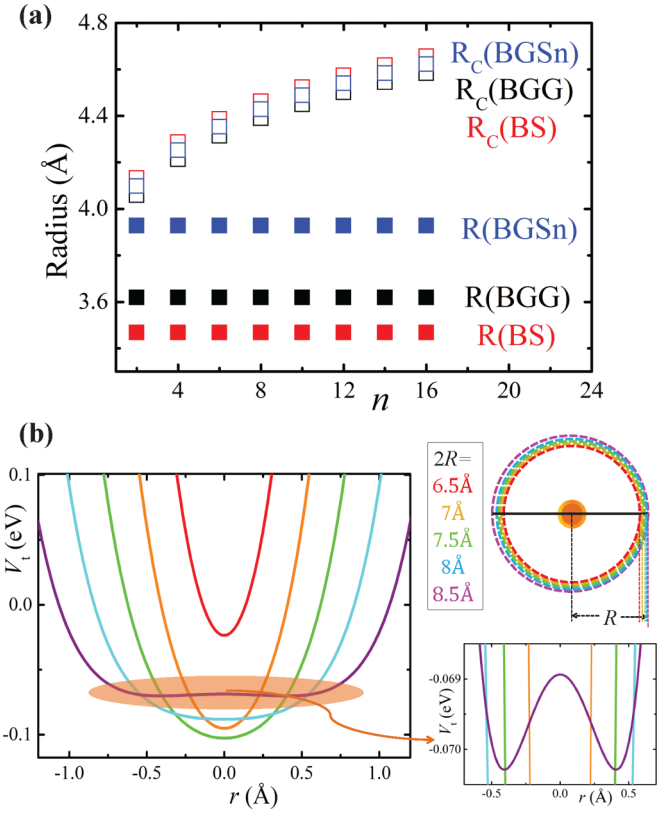

FIG. 6. Potentials. (a) A comparison between the critical radii (R_C) calculated by Eq. (9) and the cage radii (R). (b) The potential simulated according to Eq. (3). The top right corner shows the configuration in the potential model, where a guest atom is in the center and the cage atoms are on the two sides. The cage size (2R) varies from 6.5 to 8.5 Å. r_e is set to 3.67 Å, corresponding to the situation of BGSn, and n is set to the minimum value of 2. The picture at the lower right corner shows an off-centered potential when the cage radius becomes larger than R_c.

two cage atoms as shown in Fig. 6(b), the total potential $V_t(r)$ inside a cage can be described as

$$\begin{aligned} V_t(r) &= V(R+r) + V(R-r) \\ &= ae^{-nb(R+r-r_e)} - ane^{-b(R+r-r_e)} \\ &\quad + ae^{-nb(R-r-r_e)} - ane^{-b(R-r-r_e)}. \end{aligned} \tag{3}$$

According to Eq. (3), the first and the second derivatives of $V_t(r)$ are

$$\begin{aligned} V_t'(r) &= -anbe^{-nb(R+r-r_e)} + anbe^{-b(R+r-r_e)} \\ &\quad + anbe^{-nb(R-r-r_e)} - anbe^{-b(R-r-r_e)}, \end{aligned} \tag{4}$$

$$\begin{aligned} V_t''(r) &= an^2b^2e^{-nb(R+r-r_e)} - anb^2e^{-b(R+r-r_e)} \\ &\quad + an^2b^2e^{-nb(R-r-r_e)} - anb^2e^{-b(R-r-r_e)}. \end{aligned} \tag{5}$$

In the case where a guest atom is located at the center of a cage, r is equal to 0 and then we have

$$V_t(R) = 2a(e^{-nb(R-r_e)} - ne^{-b(R-r_e)}), \tag{6}$$

$$V_t'(R) = 0, \tag{7}$$

$$V_t''(R) = 2anb^2(ne^{-nb(R-r_e)} - e^{-b(R-r_e)}). \tag{8}$$

Equation (7) shows that either a potential minimum or a maximum point appears in the center of a cage. When $V_t''(R) > 0$, the central position becomes a potential minimum and stable. According to this condition, R should satisfy the following criterion:

$$R < R_c = r_e + \frac{\ln(n)}{nb - b}. \quad (9)$$

When R is larger than R_c [$V_t''(R) < 0$], the central position becomes a potential maximum and the guest atom moves towards the cage side until it reaches a stable off-center position. Since most of the type-I clathrates have on-centered guest atoms except for a few compounds like BGSn, SGG, and SGSG, which show strong anharmonicity in the phonon modes, the condition of R less than R_c can be applied. Based on the model described above, F_c can be derived from the second derivative $V_t''(R)$ in the framework of the harmonic approximation:

$$F_c = 2anb^2(ne^{nbr_e}e^{-nbR} - e^{br_e}e^{-bR}). \quad (10)$$

In principle, r_e can be estimated as $R_h + R_g$. According to Eq. (10), if r_e is fixed, which means that $R_h + R_g$ does not vary so greatly, F_c will exponentially decrease as R increases under the condition that $ne^{nbr_e}e^{-nbR} \gg e^{br_e}e^{-bR}$. This can actually be exemplified by the dotted lines in Fig. 3(c) for Ba- and Sr-inclusion clathrates, respectively. On the other hand, considering the case of the same cage, which means little variation in R, F_c should increase exponentially as r_e increases. This situation can be seen by the solid lines in Fig. 3(c) for the Si clathrates with different guest atoms. In order to achieve a unified relationship for ALE peaks appearing in clathrates, we introduced a parameter associated with the space freedom in a cage with the definition of $R_{free} = R - R_h - R_g$ as described earlier. According to the definition of r_e, R_{free} should equal to $R - r_e$, and consequently the general expression of F_c using the new parameter R_{free} becomes

$$F_c = 2anb^2(ne^{-nbR_{free}} - e^{-bR_{free}}) \cong 2an^2b^2e^{-nbR_{free}}, \quad (11)$$

where we suggest $ne^{-nbR_{free}} \gg e^{-bR_{free}}$. Actually, we have shown [Fig. 3(e)] that all F_c values can be plotted by a single exponential function, although clathrates showing off-entered guest atoms give a slightly lower F_c. It should be noted that the fitting using the two terms in Eq. (11) also gives a negligible contribution from the second term, and therefore F_c can safely be expressed as $F_c = 2an^2b^2e^{-nbR_{free}}$. When the expression of F_c is compared with the fitting result in Fig. 3(e), which shows $F_c = 0.15\exp(-3.0R_{free})$, one can evaluate $nb = 3$ Å^{-1} and $a = 8.33$ μdyn Å $= 52.1$ meV.

We tested how the model described in the present paper is applicable to the observed experimental data shown in Fig. 6(a). The critical radii (R_C) are compared with the cage radii (R) and they are plotted as a function of n for BS, BGG, and BGSn. According to Fig. 6(a), even for the smallest n, $R < R_C$. This is indicative of the fact that type-I clathrates can be classified as guest on-centered compounds as we discussed earlier.

The above situation can also be displayed as in Fig. 6(b), where the cage size ($2R$) varies from 6.5 to 8.5 Å. It is clear from this figure that the potential strongly depends upon the cage size. When the cage becomes smaller, the potential becomes sharper. When the cage becomes larger, the potentials becomes soft and flat, ending up with a symmetric two-well potential as shown in the lower right corner of Fig. 6(b). However, it should be kept in mind that R of actual type-I clathrates is always smaller than R_c under the model described above, and therefore the space found in clathrates is not large enough to allow for the appearance of off-center positions. In order to understand the off-centered situation, the space factor is not sufficient, and a lower symmetry becomes quite important as well. Typical good examples of this are BGG and SGG, as well as KGSn and BGSn. In the former case, besides the large free space of Sr inside the cage, it has also been reported that the cage structure of the two compounds is different due to the interactions between the guest atoms (Ba or Sr) and the atoms residing on the cage [54,56], and therefore off-centered Sr can be seen in SGG, while Ba is in the cage center for BGG. In the latter case, an off-centered situation can only be observed for BGSn but not for KGSn, although both clathrates have a similar cage size. Previous report showed that the difference originates from the arrangement of the cage atoms [13,45]. It is also important to point out that asymmetry of the two-well potential is necessary for the tunneling described by Anderson [58].

IV. CONCLUSIONS

We showed that the excitation energies of many ALE peaks, which are experimentally observed in type-I clathrates, can be unified as one single exponential line using a space parameter (R_{free}) associated with the freedom of motion of atoms inside the larger 24-cages. A model based on the van der Waals repulsive and attractive terms explained the intrinsic nature for the single exponential relationship between the low excitation energies and the structural factors. Discussions were made on a basis of both experimental data and theoretical calculations, and it was clarified that, in a slight contradiction of previous thought, Coulombic ionic and/or covalent interactions are not very important on the energy scale of the excitation peaks. Van der Waals type guest-host interactions, deduced from the unified picture, were suggested to be the origin of the ALE peaks appearing in clathrates with on-centered cage structure with preserved high symmetry. The consequences of these weak interatomic interactions accompanied with robust cage structure can lead to the PGEC or a recent "part-liquid part-crystalline" concept for thermoelectric applications [18,61–63]. The evolution from QH- to AH-ALE peaks can be a result of a broken or lower symmetry of the cage caused via rearrangement of the constituent elements triggered by ionic and/or covalent guest-host interactions during the formation of cage materials, in addition to a large freedom of space for the guest atoms. The influence of the lower symmetry gradually becomes evident at lower temperatures, as indicated by tunneling states. The situation discussed in the present paper from the QH to the AH modes may provide useful information for understanding the origin of ALE peaks observed in other disordered systems. In a glasslike disordered system, emergent boson peaks are suggested to be associated with localized phonons, originating from defectlike structures, which is also indicative of the importance of symmetry lowering.

ACKNOWLEDGMENTS

This work was partially supported by the AIMR collaborative research program. J.W. would like to thank MEXT for their promotion of student education through the IGPAS program. K.T. would like to thank Ryota Nakai and Masamichi Miyama for their fruitful discussion. J.X. acknowledges financial support by the National Nature Science Foundation of China (NSFC No. 11304327 and No. 11404348). The computation was done using the HA8000 system of RIIT, Kyushu University.

[1] F. Sette, M. H. Krisch, C. Masciovecchio, G. Ruocco, and G. Monaco, Science **280**, 1550 (1998).
[2] B. Frick and D. A. Richter, Science **267**, 1939 (1995).
[3] B. Hehlen, E. Courtens, R. Vacher, A. Yamanaka, M. Kataoka, and K. Inoue, Phys. Rev. Lett. **84**, 5355 (2000).
[4] U. Buchenau, Y. M. Galperin, V. L. Gurevich, and H. R. Schober, Phys. Rev. B **43**, 5039 (1991).
[5] T. Nakayama, Rep. Prog. Phys. **65**, 1195 (2002).
[6] M. Christensen, A. B. Abrahamsen, N. B. Christensen, F. Juranyi, N. H. Andersen, K. Lefmann, J. Andreasson, C. R. H. Bahl, and B. B. Iversen, Nat. Mater. **7**, 811 (2008).
[7] J. S. Tse, D. D. Klug, J. Y. Zhao, W. Sturhahn, E. E. Alp, J. Baumert, C. Gutt, M. R. Johnson, and W. Press, Nat. Mater. **4**, 917 (2005).
[8] R. P. Hermann, R. Jin, W. Schweika, F. Grandjean, D. Mandrus, B. C. Sales, and G. J. Long, Phys. Rev. Lett. **90**, 135505 (2003).
[9] H. Mutka, M. M. Koza, M. R. Johnson, Z. Hiroi, J. I. Yamaura, and Y. Nagao, Phys. Rev. B **78**, 104307 (2008).
[10] A. D. Caplin, G. Grüner, and J. B. Dunlop, Phys. Rev. Lett. **30**, 1138 (1973).
[11] A. I. Rykov, K. Nomura, T. Mitsui, and M. Seto, Physica B **350**, 287 (2004).
[12] B. C. Sales, B. C. Chakoumakos, R. Jin, J. R. Thompson, and D. Mandrus, Phys. Rev. B **63**, 245113 (2001).
[13] K. Suekuni, M. A. Avila, K. Umeo, H. Fukuoka, S. Yamanaka, T. Nakagawa, and T. Takabatake, Phys. Rev. B **77**, 235119 (2008).
[14] J. Tang, J. Xu, S. Heguri, H. Fukuoka, S. Yamanaka, K. Akai, and K. Tanigaki, Phys. Rev. Lett. **105**, 176402 (2010).
[15] J. L. Cohn, G. S. Nolas, V. Fessatidis, T. H. Metcalf, and G. A. Slack, Phys. Rev. Lett. **82**, 779 (1999).
[16] S. Pailhès, H. Euchner, V. M. Giordano, R. Debord, A. Assy, S. Gomes, A. Bosak, D. Machon, S. Paschen, and M. deBoissieu, Phys. Rev. Lett. **113**, 025506 (2014).
[17] T. Tadano, Y. Gohda, and S. Tsuneyuki, Phys. Rev. Lett. **114**, 095501 (2015).
[18] G. A. Slack, *CRC Handbook of Thermoelectrics*, edited by D. M. Rowe (CRC Press, Boca Raton, FL, 1995), pp. 407–440.
[19] H. Kawaji, H. O. Horie, S. Yamanaka, and M. Ishikawa, Phys. Rev. Lett. **74**, 1427 (1995).
[20] J. Wu, J. Xu, D. Prananto, H. Shimotani, Y. Tanabe, S. Heguri, and K. Tanigaki, Phys. Rev. B **89**, 214301 (2014).
[21] J. Xu, J. Tang, K. Sato, Y. Tanabe, H. Miyasaka, M. Yamashita, S. Heguri, and K. Tanigaki, Phys. Rev. B **82**, 085206 (2010).
[22] J. Xu, S. Heguri, Y. Tanabe, G. Mu, J. Wu, and K. Tanigaki, J. Phys. Chem. Solids **73**, 1521 (2012).
[23] U. Aydemir, C. Candolfi, A. Ormeci, Y. Oztan, M. Baitinger, N. Oeschler, F. Steglich, and Y. Grin, Phys. Rev. B **84**, 195137 (2011).
[24] M. Falmbigl, M. X. Chen, A. Grytsiv, P. Rogl, E. Royanian, H. Michor, E. Bauer, R. Podloucky, and G. Giester, Dalton Trans. **41**, 8839 (2012).
[25] K. Tanigaki, T. Shimizu, K. M. Itoh, J. Teraoka, Y. Moritomo, and S. Yamanaka, Nat. Mater. **2**, 653 (2003).
[26] P. Toulemonde, C. Adessi, X. Blase, A. San Miguel, and J. L. Tholence, Phys. Rev. B **71**, 094504 (2005).
[27] K. Suekuni, M. A. Avila, K. Umeo, and T. Takabatake, Phys. Rev. B **75**, 195210 (2007).
[28] S. Stefanoski, J. Martin, and G. S. Nolas, J. Phys. Condens. Matter **22**, 485404 (2010).
[29] M. J. Frisch *et al.*, *Gaussian 09, Revision D.01*, (Gaussian, Inc., Wallingford CT, 2009).
[30] A. D. Becke, J. Chem. Phys. **98**, 5648 (1993).
[31] C. Lee, W. Yang, and R. G. Parr, Phys. Rev. B **37**, 785 (1988).
[32] V. A. Rassolov *et al.*, J. Comp. Chem. **22**, 976 (2001).
[33] P. J. Hay and W. R. Wadt, J. Chem. Phys. **82**, 299 (1985).
[34] G. Kresse and J. Furthmuller, Phys. Rev. B **54**, 11169 (1996).
[35] P. E. Blochl, Phys. Rev. B **50**, 17953 (1994).
[36] G. Kresse and D. Joubert, Phys. Rev. B **59**, 1758 (1999).
[37] J. P. Perdew, K. Burke, and M. Ernzerhof, Phys. Rev. Lett. **77**, 3865 (1996).
[38] T. Takabatake, K. Suekuni, T. Nakayama, and E. Kaneshita, Rev. Mod. Phys. **86**, 669 (2014).
[39] T. Nakayama and E. Kaneshita, Europhys. Lett. **84**, 66001 (2008).
[40] T. Kume, H. Fukuoka, T. Koda, S. Sasaki, H. Shimizu, and S. Yamanaka, Phys. Rev. Lett. **90**, 155503 (2003).
[41] D. Nataraj and J. Nagao, J. Solid State Chem. **177**, 1905 (2004).
[42] S. Johnsen, M. Christensen, B. Thomsen, G. K. H. Madsen, and B. B. Iversen, Phys. Rev. B **82**, 184303 (2010).
[43] H. Shimizu, Y. Takeuchi, T. Kume, S. Sasaki, K. Kishimoto, N. Ikeda, and T. Koyanagi, J. Alloys Compd. **487**, 47 (2009).
[44] M. Christensen, S. Johnsen, F. Juranyi, and B. B. Iversen, J. Appl. Phys. **105**, 073508 (2009).
[45] T. Tanaka, T. Onimaru, K. Suekuni, S. Mano, H. Fukuoka, S. Yamanaka, and T. Takabatake, Phys. Rev. B **81**, 165110 (2010).
[46] T. Kume, T. Koda, S. Sasaki, H. Shimizu, and J. S. Tse, Phys. Rev. B **70**, 052101 (2004).
[47] H. Shimizu, T. Imai, T. Kume, S. Sasaki, A. Kaltzoglou, and T. F. Fassler, Chem. Phys. Lett. **464**, 54 (2008).
[48] J. M. Hutson, J. Chem. Phys. **96**, 6752 (1992).
[49] J. O. Halford, J. Chem. Phys. **24**, 830 (1956).
[50] R. H. Stokes, J. Am. Chem. Soc. **86**, 979 (1964).
[51] M. J. Mantina, A. C. Chamberlin, R. Valero, C. J. Cramer, and D. G. Truhlar, Phys. Chem. A **113**, 5806 (2009).
[52] A. Bondi, J. Phys. Chem. **68**, 441 (1964).
[53] C. Gatti, L. Bertini, N. P. Blake, and B. B. Iversen, Chem. Eur. J. **9**, 4556 (2003).

[54] D. Arcon, A. Zorko, P. Jeglic, J. Xu, J. Tang, Y. Tanabe, S. Heguri, and K. Tanigaki, J. Phys. Soc. Jpn. **82**, 014703 (2013).
[55] H. Zhang, H. Borrmann, N. Oeschler, C. Candolfi, W. Schelle, M. Schmidt, U. Burkhardt, M. Baitinger, J. Zhao, and Y. Grin, Inorg. Chem. **50**, 1250 (2011).
[56] J. Tang, T. Rachi, R. Kumashiro, M. A. Avila, K. Suekuni, T. Takabatake, F. Z. Guo, K. Kobayashi, K. Akai, and K. Tanigaki, Phys. Rev. B **78**, 085203 (2008).
[57] T. Keiber, P. Nast, S. Medling, F. Bridges, K. Suekuni, M. A. Avila, and T. Takabatake, J. Mater. Chem. C **3**, 10574 (2015).
[58] P. W. Anderson, B. I. Halperin, C. M. Varma, Philos. Mag. **25**, 1 (1972).
[59] A. I. Chumakov, G. Monaco, A. Monaco, W. A. Crichton, A. Bosak, R. Ruffer, A. Meyer, F. Kargl, L. Comez, D. Fioretto, H. Giefers, S. Roitsch, G. Wortmann, M. H. Manghnani, A. Hushur, Q. Williams, J. Balogh, K. Parlinski, P. Jochym, and P. Piekarz, Phys. Rev. Lett. **106**, 225501 (2011).
[60] P. M. Morse, Phys. Rev. **34**, 57 (1929).
[61] H. Liu, X. Shi, F. Xu, L. Zhang, W. Zhang, L. Chen, Q. Li, C. Uher, T. Day, and G. J. Snyder, Nat. Mater. **11**, 422 (2012).
[62] D. J. Voneshen, K. Refson, E. Borissenko, M. Krisch, A. Bosak, A. Piovano, E. Cemal, M. Enderle, M. J. Gutmann, M. Hoesch, M. Roger, L. Gannon, A. T. Boothroyd, S. Uthayakumar, D. G. Porter, and J. P. Goff, Nat. Mater. **12**, 1028 (2013).
[63] W. Qiu, L. Xi, P. Wei, X. Ke, J. Yang, and W. Zhang, Proc. Natl. Acad. Sci. USA **111**, 15031 (2014).